Citation: Journal of Optics 16 125713 (2014)
https://doi.org/10.1088/2040-8978/16/12/125713

Reflective and transmissive broadband coating polarizers in a spectral range centered at 121.6 nm

Juan I. Larruquert[1a], A. Marco Malvezzi[2,3,5], Angelo Giglia[3], José A. Aznárez[1], Luis Rodríguez-de Marcos[1], José A. Méndez[1], Paolo Miotti[4], Fabio Frassetto[4], Giuseppe Massone[5], Stefano Nannarone[3], Giuseppe Crescenzio[5], Gerardo Capobianco[5], Silvano Fineschi[5]

[1]GOLD, Instituto de Óptica-Consejo Superior de Investigaciones Científicas, Madrid, Spain

[2]Universitá di Pavia, Pavia, Italy

[3]Istituto Officina dei Materiali -Consiglio Nazionale delle Ricerche, Trieste, Italy

[4]Institute of Photonics and Nanotechnologies-National Council for Research, Padua, Italy

[5]INAF - Osservatorio Astrofisico di Torino, Torino, Italy

ABSTRACT

Polarimetry is a powerful tool for the interpretation of the role of the coronal plasma in the energy transfer processes from the inner parts of the Sun to the outer space. One of the key lines for observations is H I Lyman α (121.6 nm) among few spectral lines in the far ultraviolet (FUV), and hence efficient linear polarizers at this line are demanded. New designs based on $(Al/MgF_2)_n$ multilayer coatings have been developed to obtain the smallest possible reflectance in the parallel plane of polarization (R_{par}) with a simultaneous high reflectance in the perpendicular plane of polarization (R_{per}). Samples stored in nitrogen for ~8-17 months resulted in efficient polarizers at 121.6 nm, with R_{par}~0.01-0.017 and R_{per}~0.69-0.725. The designs with a number n=3 to 4 bilayers of Al/MgF_2 result in a wider spectral range of efficient linear polarizers, compared to what can be obtained with n=2. Coatings following various designs with good polarizing performance in a 7-to-8-nm wide FUV range were prepared. For the first time, a transmissive coating polarizer has been developed for this range, which has the benefit that it involves no deviation of the beam; it is based on another design of $(Al/MgF_2)_3$ multilayer coating. The transmissive polarizer has a good transmittance ratio between the two polarization components and, even though its figure of merit is not as high as

[a] larruquert@io.cfmac.csic.es; phone: 34- 915618806 ext 330; fax: 34-914117651

that of the reflective polarizers, it incorporates filtering properties to reject wavelengths both below and above 121.6 nm; this property might enable a polarimeter for solar physics with an improved global figure of merit if a filter to isolate the H I Lyman α line could be avoided.

I. INTRODUCTION

In the solar chromosphere and corona, the magnetic field controls the structure and dynamics of the atmosphere. In these high-temperature ($10^4 – 10^6$ K) outer layers, strong resonance lines are formed in the ultraviolet (UV) wavelength region (10 – 100 nm). In the solar chromosphere (i.e., $10^0 – 10^1$ Mm, above the photosphere) magnetic fields of the order of $10^2 – 10^3$ G can be diagnosed by polarimetric observations of the Zeeman effect in UV lines. In the inner solar corona (i.e., $10^2 – 10^3$ Mm, above the photosphere), and in the outer solar and stellar envelopes ($\geq 10^4$ Mm), the Zeeman effect will not be observable because the magnetic fields are weaker ($< 10^2$ G) than those in the photosphere and in the chromosphere. As a consequence, the Doppler broadening, due to the higher temperatures of these layers (10^6-10^7 K), blends the Zeeman split components.

In the solar corona and stellar envelopes, line scattering polarization can be modified by magnetic fields through the Hanle effect. This effect can be observed because Doppler broadening does not cancel scattering polarization. So, for temperatures typical of the solar corona and hot stars, the Hanle effect in far UV (FUV, here 90 nm$<\lambda<$200 nm) line polarization is expected to be a viable diagnostic of magnetic fields in the range of 10^0 - 10^2 G [1].

Solar UV polarimetry from space was pioneered by a Swedish-built UV spectropolarimeter launched in 1976 on a Soviet Intercosmos satellite [2]. The instrument was designed to record resonance-line polarization in the FUV wavelength region 120 – 150 nm of the chromospheric spectrum. This was the first demonstration of the feasibility of FUV polarization measurement in an astronomical source. After this, the Ultraviolet Spectrometer and Polarimeter (UVSP) of the Solar Maximum Mission (SMM) [3] provided the first polarimetric measurements in the solar spectrum below 200 nm. SUMER/SOHO has probed the coronal magnetic fields via the Hanle effect on FUV resonance-line polarization of O VI, 103.2 nm [4]. The FUSP sounding-rocket payload is designed for measurements of the Hanle effect in FUV resonance lines

from hot stars envelopes [5]. The Solar Ultraviolet Magnetograph Investigation (SUMI) sounding-rocket payload is an instrument that measures the polarization in the UV lines of Mg II 280 nm and C IV 154.8 nm formed in the transition region and upper chromosphere [6].

These past missions have sparked interest for solar and stellar FUV polarimetry and new, more efficient FUV polarizers will be needed for the new missions that have been recently proposed, such as for instance COMPASS and SolmeX [7] and CLASP [8]. The most interesting FUV wavelength range for the diagnostics of solar and stellar magnetic fields via spectral-line-polarimetry of the Zeeman and Hanle effects is the 90-150 nm interval. In this spectral range many hydrogen-like emission lines are formed in the hot (10^4-10^7 K) astrophysical plasmas, in particular the neutral hydrogen (HI) Lyman-series lines and the O VI and C IV lines.

Efficient polarizers at H Lyman α at 121.6 nm and at close spectral lines like H Lyman β (102.6 nm) and O VI (103.2 and 103.8 nm) are necessary for polarimetric observations of the solar corona. Light emitted and/or scattered at those wavelengths by ions in the solar corona is partially polarized, and the measurement of that partial polarization may provide valuable information.

Reflective polarizers for 121.6 nm and shorter FUV wavelengths have been most often based on the reflection on a plate at an angle close to Brewster angle; at this angle, the polarization component within the plane of incidence is virtually zero, i.e., $R_p \approx 0$, whereas the other component, R_s, is desired to be as high as possible, but usually it reaches modest values. Reflection polarizers are then good at rejecting one component. Plates must be made of basically transparent materials, most often LiF and MgF_2 [9,10,11,12,13], along with few other materials like fused silica [14], micaceous biotite [15], diamond [5,16], CaF_2, pyrex, or corundum [17]. Coatings have been also used to make polarizers, both by reflection at a single mirror [18,19,20,21] and also at a 3-mirror [22,23,24,25,26,27] or 4-mirror [28] configuration to keep the optical axis unmoved, although the latter configurations result in low-efficiency polarizers that besides are difficult to align.

The advantage of coatings versus transparent plates is that the designer has some degrees of freedom to get a high R_s/R_p ratio while increasing R_s above the modest value that can be obtained with a plate at Brewster angle. Multilayer coatings based on Al and

MgF_2 are a good choice for polarizers at 121.6 nm because of the high intrinsic reflectance of Al, the minimum absorption of MgF_2, and their large refractive index contrast. Kim et al. [29] designed polarizers working at either 121.6 nm or 130.4 nm and at 45° angle based on an $(Al/MgF_2)_2$ multilayers. Bridou et al. [21] designed and succeeded in preparing various sorts of coatings designed for optimum polarization performance at 121.6 nm; the coating based on an $(Al/MgF_2)_2$ multilayer had the largest R_s among the different coatings.

Even though polarizers at Brewster angle are good at rejecting one polarization component when they operate by reflection, this property has been often used in the reverse way, i.e., by transmission, due to the benefit of not bending the optical axis. In transmission, since the T_p/T_s ratio is not large, a series of inclined plates are often used to enhance this number; the drawback of this is that the combined transmittance at the passing polarization component is usually small. In transmission mode, a pile of plates of LiF [30,31,32,33] has been most often used, although MgF_2 has been also used in spite of its residual birefringence at 121.6 nm and shortwards [34]. To our knowledge, transmissive polarizers based on coatings have not been developed for these wavelengths yet. Further information can be found in the various reviews of devices and coatings used for linear polarizers in the FUV and extreme UV [35,36,37].

This research presents new polarizers based on $(Al/MgF_2)_3$ and $(Al/MgF_2)_4$ multilayer coatings that cover a certain spectral range around 121.6 nm. Section II outlines the experimental techniques for coating preparation and polarization measurements used in this research. Section III presents the designs and the reflectance or transmittance measurements for the two polarization components on various coating polarizers as a function of wavelength and incidence angle, along with measurements on aged coatings.

II. EXPERIMENTAL TECHNIQUES

A. Coating preparation

$(Al/MgF_2)_3$ and $(Al/MgF_2)_4$ multilayer coatings (Al is the innermost layer and MgF_2 is the outermost one) were deposited at GOLD in a 50-cm-side cubic, high-vacuum chamber. The chamber was pumped with a turbomolecular system and a liquid-N_2 cooled, Ti sublimation pump. Both Al and MgF_2 films were deposited by evaporation using W boats (MgF_2) and filaments (Al). 99.999% pure Al and VUV-grade MgF_2 were used as evaporant materials; the deposition rate was ~1.0 nm/s for Al and ~0.7 nm/s for

MgF_2. The base pressure in the chamber was 10^{-5} Pa.; pressure increased during deposition to ~10^{-4} Pa (Al) and ~5×10^{-5} Pa (MgF_2). Substrates were pieces of polished float glass (reflective polarizers) or MgF_2 crystals cut perpendicular to the c-axis (transmissive polarizers), which were not intentionally heated or cooled during or after deposition. The distance between the evaporation source and the substrate was 30 cm. Film thickness was measured with a quartz-crystal monitor, that had been calibrated through Tolansky interferometry, i.e., through multiple-beam interference fringes in a wedge between two highly reflective surfaces [38]. Before the initial measurements, samples were kept in residual vacuum most of the time after preparation, and the total exposure to the atmosphere was approximately one week. After the initial measurements were completed, samples were stored in a box filled with nitrogen and were kept there for months until they were taken out to measure them again.

B. Reflectance/transmittance measurements

Polarization performance was measured at Bending magnet for Emission, Absorption and Reflectivity (BEAR) beamline of ELETTRA synchrotron (Trieste, Italy) [39,40,41]. During reflectance or transmittance measurements, we used a 0.5-mm thick LiF crystal made by Crystec for higher order rejection. Measurements were performed with exit slits opened at 900x400 μm^2; with this configuration the spot size on the sample was 400x400 μm^2 and the bandwidth was 0.060 eV FWHM. The detector was a silicon diode IRD-SXUV100; the background was subtracted for each measurement. In order to improve accuracy, each measurement was made up by 5 signal measurements and 5 successive background measurements repeated up to 15 times for each energy point. Both for transmittance and reflectance measurements, the beam impinged on the sample from the coating side.

Measurements with polarized radiation are possible due to the polarization properties of the bending magnet source, which depend on the emission angle. Radiation is linearly polarized in the storage ring plane and elliptically polarized outside. The polarization state of the light can be selected with the polarization selector, a double slit device that can be regulated to define the vertical acceptance of the bending magnet source. Measurements have been made in linear polarization configuration, i.e. with the polarization selector centered with respect to the beam source in the vertical direction (perpendicular to the ring plane). The selector slits were set to have a calculated degree of linear polarization of the beam of approximately $(I_s-I_p)/(I_s+I_p)=0.99$, where I_s and I_p

stand for the incident beam intensity with the electric vector perpendicular and parallel, respectively, to the plane of incidence. This corresponds to a vertical acceptance of 4 mm and to an angular aperture of ±0.17 mrad. Reflectance/transmittance measurements were performed in two perpendicular planes of incidence, for which the experimental chamber was rotated 90° around the beam axis. The role of s and p are interchanged when the chamber rotates 90°.

III. RESULTS AND DISCUSSION

A. Reflective polarizers

In the literature, reflective polarizers based on $(Al/MgF2)_2$ multilayers have been proposed [29] and prepared [21]. The present design of polarizers attempted to get the largest efficiency in the broadest possible spectral range. This led us to design multilayers with the largest possible degrees of freedom, i.e., the number of layers with their thicknesses to be optimized. Fig. 1 displays calculated R_p and R_s of designs with 2, 3, and 4 Al/MgF_2 bilayers optimized to have a polarizer in the spectral range around 121.6 nm; the coatings are designed to operate at 65°. The increase in the number of bilayers results in a polarizer with a larger spectral range of operation. The larger range of operation not only increases the scope of application of the coatings but it is expected to result in coatings that are less affected by residual layer thickness errors.

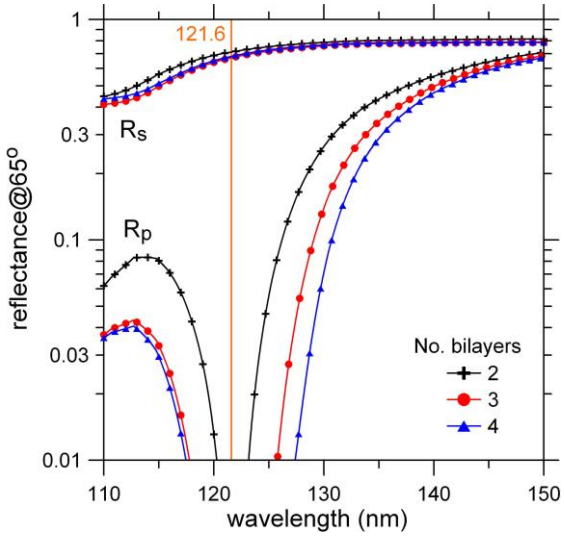

Fig. 1. Calculated log-axis R_p and R_s at 65° versus wavelength for polarizer coating designs with 2, 3, and 4 Al/MgF_2 bilayers

The performance of three reflective polarizers prepared in this research is presented below. The design of these polarizers is given in Table 1. Sample R1 was designed with 4 bilayers, whereas samples R2 and R3 were designed with three bilayers; each design was optimized at a specific incidence angle.

Table 1. Optimization angle (from the normal) and optical layer thicknesses (in quarterwaves) of the present multilayer coatings; 1: innermost bilayer; 4: outermost bilayer

Sample	Opt. angle	Optical layer thickness (quarterwaves)							
		Al 1	MgF_2 1	Al 2	MgF_2 2	Al 3	MgF_2 3	Al 4	MgF_2 4
R1	69°	0.030	0.26	0.013	0.25	0.010	0.28	0.005	0.59
R2	60°	0.035	0.33	0.019	0.37	0.006	0.65		
R3	65°	0.029	0.28	0.015	0.31	0.005	0.62		
T1	78°	0.002	0.13	0.003	0.11	0.003	0.32		

Coating polarizers were prepared and measured for successive measurement campaigns at BEAR-ELETTRA. Hence the results obtained in one campaign helped refine the designs for the next campaign. For sample R2, Fig. 2 displays contour plots of both R_{par} and R_{per} (R_{par} and R_{per} are the reflectance measured in a plane that is parallel and perpendicular, respectively, to the storage ring) as a function of wavelength and angle of incidence; these are the initial measurements taken on R2 after 7 weeks of storage in residual vacuum plus ~1 week of storage in air. Measurements were performed in an extended spectral and angular range in order to explore their full potential as polarizers. In the R_{par} plot there is a central area under 0.01 covering the 119.6-129-nm range with angles in the ~62°-70° range. At this central area, R_{per} approaches or surpasses 0.70. There are two secondary low-R_{par} areas centered at 115 nm (R_{per}~0.60-0.80) and at 133 nm (R_{per}~0.70-0.80) in the 76°-80° range. A wide spectral range of ~113-134 nm can be covered with this polarizer by selecting the optimum incidence angle.

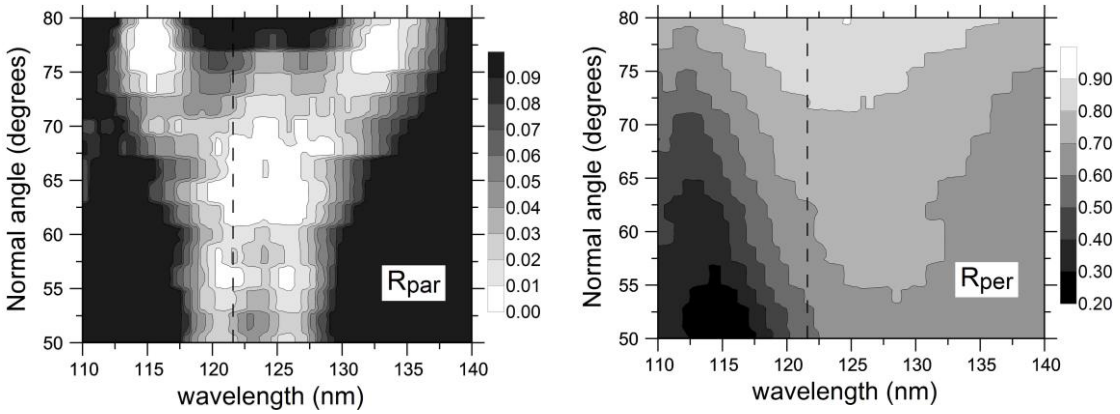

Fig. 2. Contour plot of R_{par} (left) and R_{per} (right) as a function of wavelength and angle of incidence (measured from the normal) of sample R2 in the initial measurements after deposition. The dashed line represents the target wavelength of 121.6 nm.

In ideal conditions, R_{par} and R_{per} would be equivalent to R_p and R_s, respectively. In practice, full light polarization is only available in the exact storage ring plane; however, in order to have a sufficient number of photons, a beam with some extension in the direction perpendicular to the storage ring must be used for measurements, which results in a beam with some residual elliptical polarization. The degree of polarization of the incoming beam, as it leaves the ring, may be slightly modified by the beamline optics and by some slight deviation of the measurement planes with respect to the storage ring plane (or its perpendicular). Hence the present R_{par} and R_{per} measurements are expected to be a higher and a lower limit, respectively, of the real R_p and R_s, or in other words, real R_s and mainly R_p are expected to give an even better performance than what is plotted in Fig. 2 and in the following figures. A comprehensive description of the polarization of synchrotron radiation can be found in the literature [42].

Fig. 3 displays R_{par} and R_{per} measured for sample R2 after 8 months **of** storage in nitrogen; the aged sample was measured at three incidence angles. R_{par} was slightly less than 0.01 at 121.6 nm for 60° and 65°, with a value of R_{per} as large as 0.69 at 65°. Best performance is obtained at 65° in the range of ~120.8-128 nm.

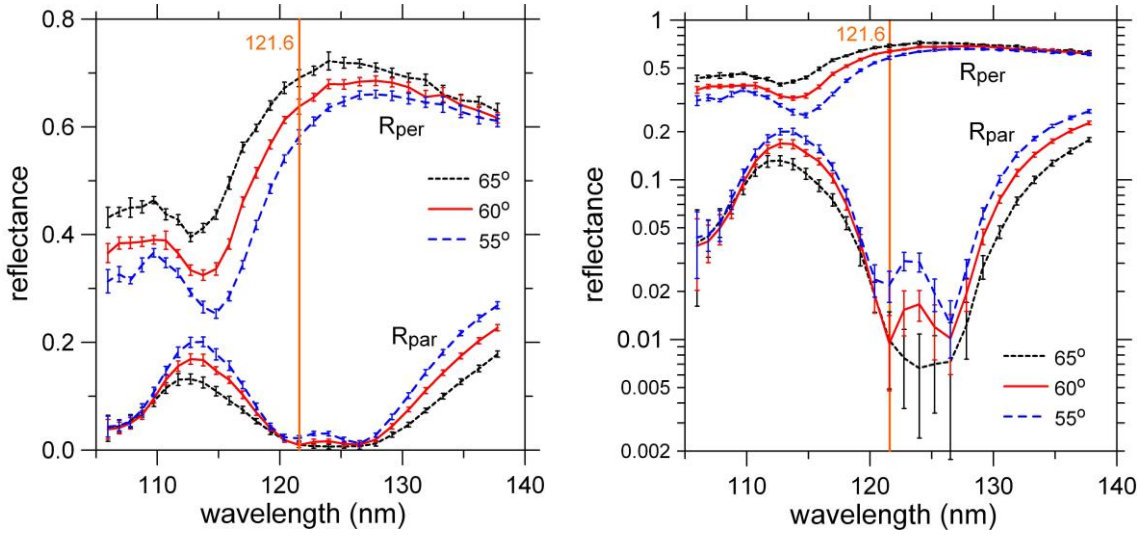

Fig. 3. Linear (left) and log-axis (right) plot of R_{par} and R_{per} versus wavelength for sample R2 aged of 8 months in nitrogen (plus seven weeks in residual vacuum) for three angles of incidence (measured from the normal)

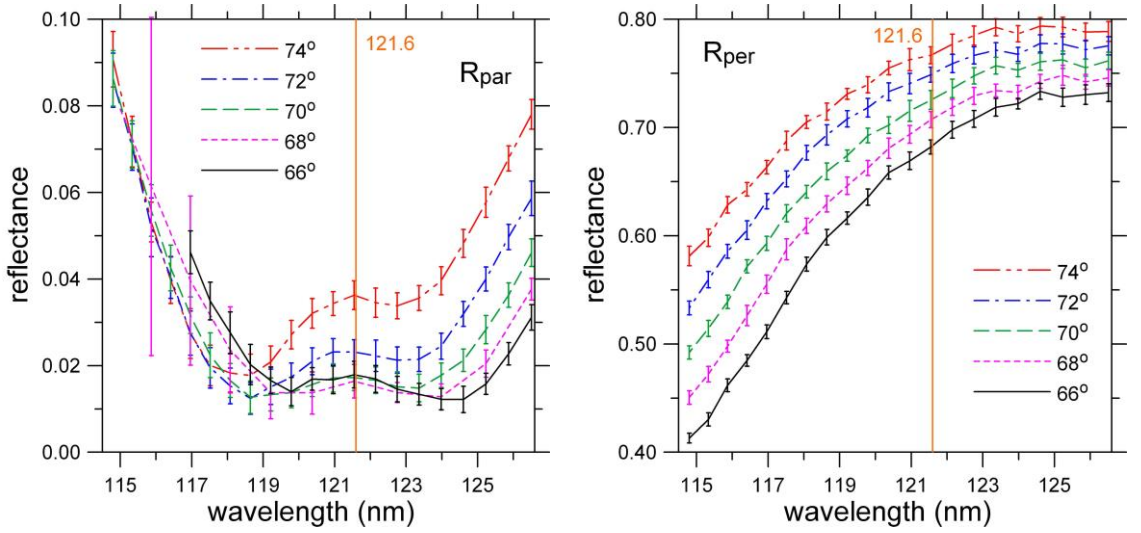

Fig. 4. R_{par} (left) and R_{per} (right) as a function of wavelength for sample R3 aged of 13 months in nitrogen. Measurements are at five incidence angles (measured from the normal)

Fig. 4 displays R_{par} and R_{per} measured for sample R3 after 13 months of storage in nitrogen; measurements were performed as a function of wavelength at five incidence angles. At 121.6 nm, R_{par}=0.017 and R_{per}=0.725 were measured at 70°. A value of R_{par} below 0.02 was measured for this sample at some incidence angle in the 117.5-125.6-nm spectral range; corresponding R_{per} stands at 0.70 and above.

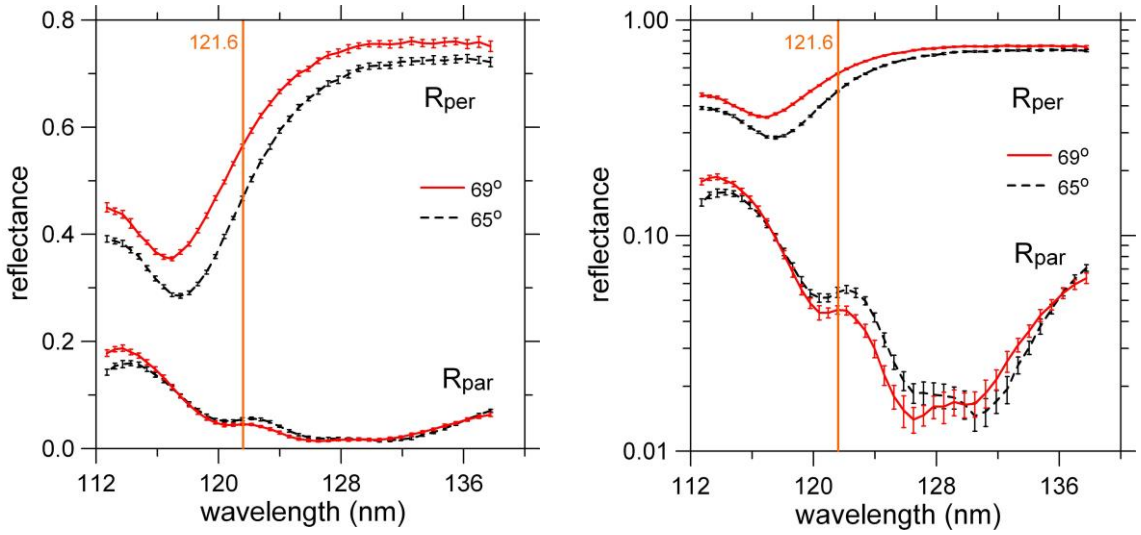

Fig. 5. Linear (left) and log-axis (right) plot of R_{par} and R_{per} versus wavelength for sample R1 aged of 17 months in nitrogen for two angles of incidence (measured from the normal)

Fig. 5 displays R_{par} and R_{per} measured for sample R1 after 17 months of storage in nitrogen; measurements were performed as a function of wavelength at two incidence angles. For this sample best polarizing properties are at wavelengths longer than 121.6 nm. This shift is attributed to films somewhat thicker than the nominal values; this sample was prepared in an earlier campaign than R2 and R3, and the shift was modeled to correct the film thicknesses in the later samples. For R1, a value of R_{par} below 0.02 was measured at some incidence angle in the 125-132.6-nm spectral range; corresponding R_{per} stands in the 0.67-0.75 range. The difference in sample storage time over the three measured samples is not expected to result in a significant difference on reflectance.

Aged samples R2 and R3, consisting of $(Al/MgF_2)_3$ coatings, result in a somewhat better performance at 121.6 nm than coatings based on the design $(Al/MgF_2)_2$ [21]; compared with the coatings with two bilayers, sample R2 has a lower R_p with the same R_s, whereas sample R3 has a larger R_s while R_p is in the short edge of the reported range of values. The present values are for aged samples whereas information on polarizer ageing was not given in Ref. 21. Additionally, polarizing properties are found here in a spectral range that extends both below and above 121.6 nm. As mentioned above, the extension of the polarizing capacity to a wider spectral range was introduced in the design with the increase of the number of bilayers.

We evaluate the efficiency of a polarizer in providing linearly polarized light in terms of the modulation factor:

$$\mu = \frac{R_s - R_p}{R_s + R_p} \tag{1}$$

Fig. 6 plots μ for the aged polarizers, where R_s and R_p were replaced with R_{per} and R_{par}. The most valuable ranges are those where μ approaches 1, with the largest possible R_s simultaneously. A useful parameter encompassing these two quantities is called the figure of merit κ, which is defined as [43]:

$$\kappa = \mu\sqrt{R} \tag{2}$$

where R is the reflectance averaged over the two polarizations: $R=(R_s+R_p)/2$, which will be referred to as throughput. κ provides information on the trade-off between polarization efficiency and throughput. We want κ to be as large as possible, keeping in mind that the maximum possible κ value (for a perfect polarizer) is $1/2^{0.5}= 0.71$. Fig. 6 displays also κ for the aged polarizers.

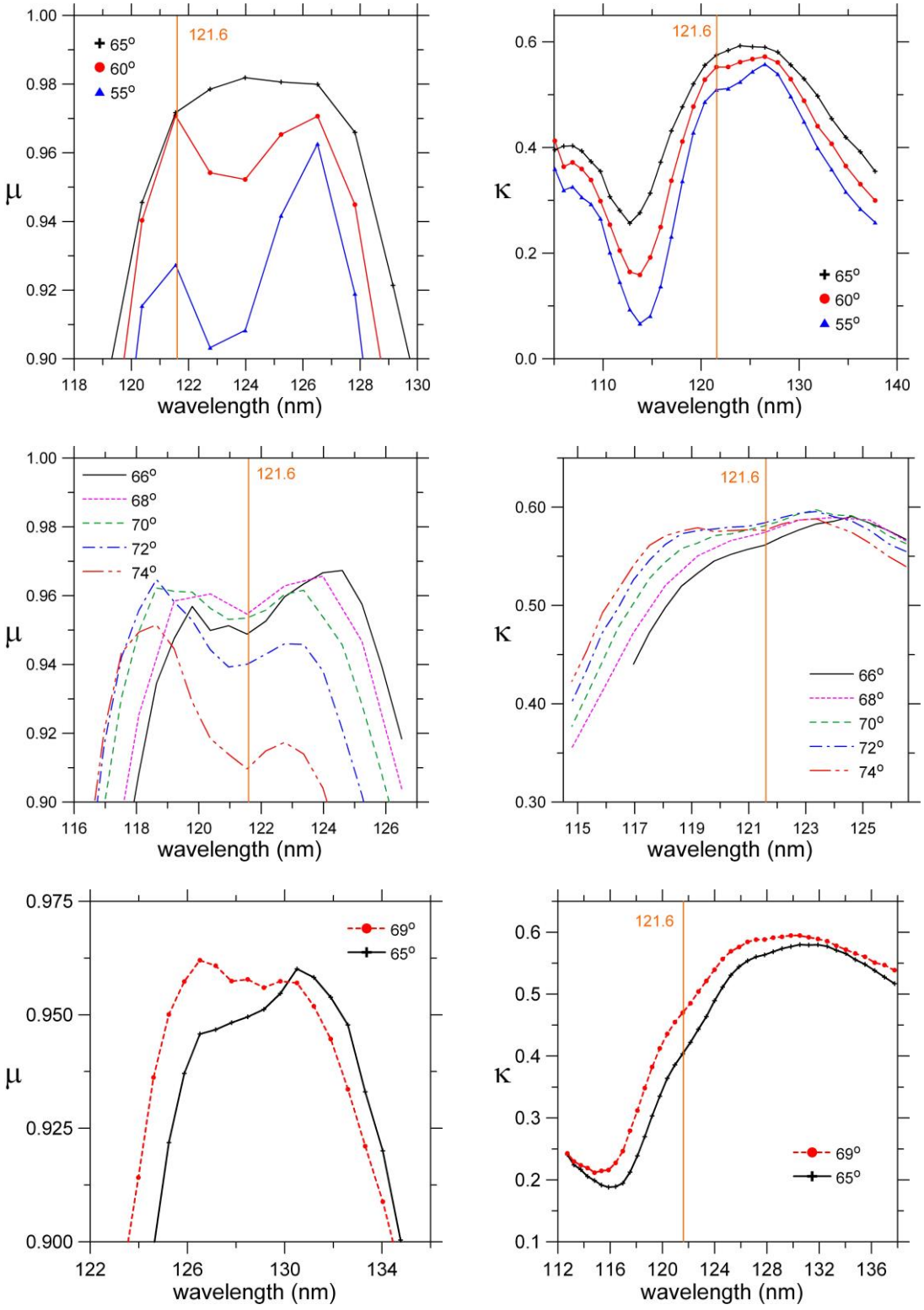

Fig. 6. μ (left) and κ (right) versus wavelength for aged samples: R2 (top), R3 (center), and R1 (bottom)

Using μ as an evaluation parameter, the best polarizer at 121.6 nm is R2 at 60°-65° with μ=0.972, but R3 is only slightly below that at 68°-70°; however, using κ as the evaluation parameter, sample R3 at 70°-72° with κ=0.584 is slightly better than sample R2, with the highest value at 65°. The largest μ over the whole set of samples, wavelength, and angles is 0.982 for sample R2 at 124.0 nm and 65°, whereas the top measured κ value is 0.597 for sample R3 at 123.4 nm and 70°, with close values for the other two samples at their optimum wavelength and angle.

B. Transmissive polarizers

The same combination of materials was used to design polarizers operating by transmission. The first benefit of these devices is that there is no deviation of the beam (except for a minor lateral shift), which can simplify an instrument operating with a transmissive polarizer. Here we used a MgF_2 substrate because the retardation due to MgF_2 birefringence is introduced after the beam has crossed the coating, so that it does not result in an intensity change on the detector. To use the polarizer in a polarimeter, a LiF substrate could be used for being non-birefringent; a MgF_2 substrate could be also used if cut with the optics axis along the beam propagation direction in the material.

Fig. 7 displays T_{per} and T_{par} measured for sample T1 after 13 months of storage in nitrogen; sample design is given in table 1 and the optimization angle is 78°. Measurements were performed as a function of wavelength at 73° and at 78°. With transmissive polarizers, the role played by the two polarization components is inverted: now the perpendicular component is more suitable to be minimized. At 121.6 nm, T_{per} and T_{par} were in the range of 0.005-0.008 and 0.096-0.11, respectively. Maximum polarization efficiency is obtained in the ~124-129-nm range. Some shift of the polarization range is observed between the two measured incidence angles; an advantage of a transmissive polarizer is that it can be somewhat tuned in wavelength by rotation**,** with no essential beam shift and no deviation. Fig. 8 plots μ and κ for the aged transmissive polarizer. The definition of throughput and of μ and κ given in Eqs. (1) and (2) has been adapted here by replacing R with T and by interchanging s and p. To our knowledge, this is the first time a transmissive coating polarizer is developed in this spectral range.

A further important benefit of the present transmissive polarizer is that it displays filtering properties, with a peak transmittance wavelength not far from 121.6 nm. In the

present design, the filtering was obtained by serendipity**,** since no requirement for filtering was included in the design. No measurement was performed outside the displayed data but calculations predict a 121.6-to-200 nm transmittance ratio of ~7. Available transmittance filters tuned around 121.6 nm and working at normal incidence have a somewhat larger transmittance ratio at these same wavelengths, in the order of 20 for a filter with a transmittance peak of 0.20. Beyond 200 nm, the off-band suppression is most often achieved by the use of solar blind UV detectors systems that are used in the FUV space instrumentation, with a negligible sensitivity beyond 200 nm.

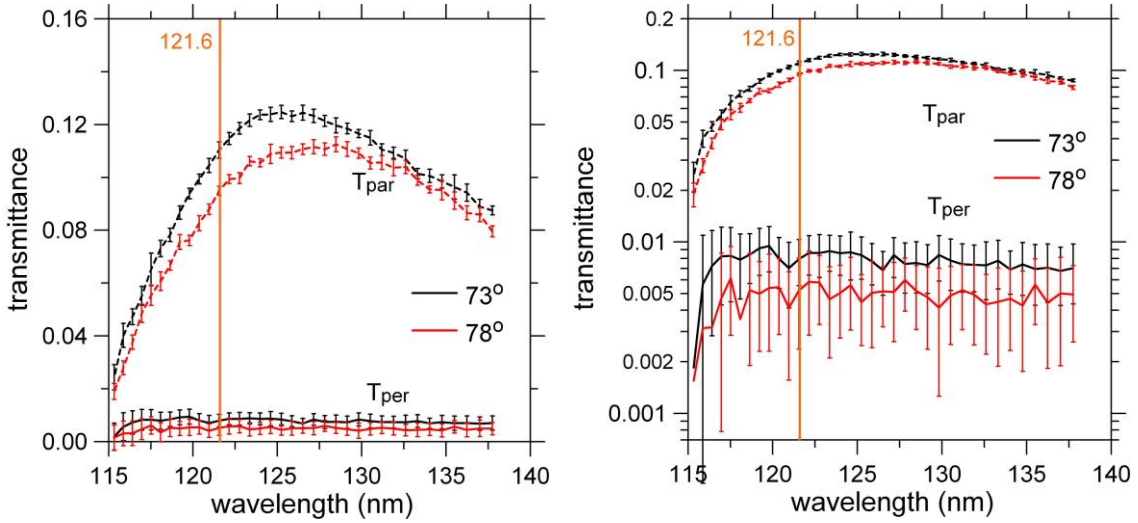

Fig. 7. Linear (left) and log-axis (right) plot of T_{per} and T_{par} versus wavelength for sample T1 aged of 13 months in nitrogen (plus two weeks in residual vacuum) for two angles of incidence (measured from the normal)

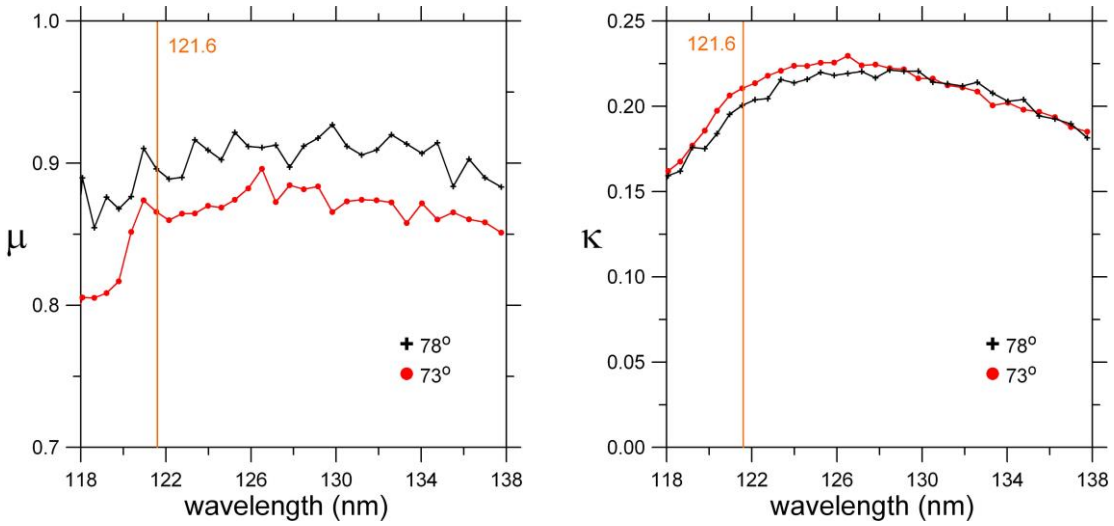

Fig. 8. μ (left) and κ (right) versus wavelength for aged T1 sample

Table 2. Comparison of the performances at 121.6 nm for different types of polarizers[a]

Principle	Coating/ Bulk	Angle of incidence	Figure-of-merit κ	Through-put	Modulation factor μ
Reflect-ance	$(Al/MgF_2)_3$ (present, R3)	70°	0.581 [0.260][b]	0.371 [0.074][b]	0.954
	$(Al/MgF_2)_3$ (present, R2)	65°	0.575 [0.257][b]	0.355 [0.071][b]	0.972
	$(Al/MgF_2)_2$ (Ref. 21, Me0808)	66°	0.552 [0.247][b]	0.360 [0.072][b]	0.92
	MgF_2/SiO_2 (Ref. 21, Me0811)	68°	0.486 [0.217][b]	0.262 [0.052][b]	0.95
	Uncoated Bulk MgF_2[43]	58° (Brewster angle)	0.34 [0.15][b]	0.12 [0.024][b]	0.99
	uncoated Au[43]	55° (pseudo-Brewster angle)	0.31 [0.14][b]	0.2 [0.04][b]	0.70
Transmit-tance	$(Al/MgF_2)_3$ (present, T1)	73°	0.211	0.0591	0.866

a: present polarizers were stored 8 to 17 months in nitrogen

b: numbers in brackets include the transmittance of a bandpass filter evaluated at 0.2

Table 2 summarizes the performances at 121.6 nm of the developed reflective and transmissive polarizers described in this paper. For comparison, the table includes also the performances of other reflective polarizers: the classical bulk MgF_2 at Brewster angle (Ref. 43), and a single Au layer coating at the so called "pseudo-Brewster" angle (Ref. 43), along with two multilayer coatings (Ref 20). In table 2, the throughput and the figure of merit appears both with its real figure and also modified to include the transmittance of a filter tuned at 121.6 nm; the modified numbers are presented in square brackets. The filter transmittance has been evaluated as 0.2 (the applied factor for the figure of merit is $\sqrt{0.2}$). The present transmittance filter is assumed not to require such a filter. This makes its performance very competitive even compared to the multilayer-coating reflective polarizers, with the advantage that transmissive polarizers do not deviate the beam. In this comparison the assumption that the present transmissive polarizer does not require a filter is speculative since no measurement was performed at long wavelengths; on the other hand, there may be room to increase the filtering properties of the polarizer if this requirement were introduced in the design.

Summarizing, a transmissive polarizer, assuming some room for increasing its filtering properties and used in conjunction with solar-blind detectors, might match the performance of a reflective polarizer that requires the addition of a UV bandpass filter.

Conclusions

Linear polarizers with three and four Al/MgF_2 bilayer coatings have been developed for H Lyman α line at 121.6 nm and the close spectral range. The use of a number of bilayers larger than two results in a polarizer with a larger spectral range of operation. Polarizers operating both by reflectance and by transmittance were developed. Polarizing properties have been obtained in a spectral range around 121.6 nm. Reflective polarizers following three different designs resulted in a high performance in the ranges of 120.8-128 nm, 117.5-125.6 nm, and 125-132.6 nm; wider polarization ranges could be possible by tuning the incidence angle. Reflective polarizers aged for 8 to 17 months in nitrogen kept R_{par} values in the 0.01-0.02 range with a simultaneous R_{per} of 0.69-0.725 at 121.6 nm. The present coatings with three Al/MgF_2 bilayers have a larger figure of merit at 121.6 nm than previous polarizers with two bilayers. Furthermore, the multilayer-coated reflective polarizers have a considerably larger performance at 121.6 nm than the classical polarizers used as reference.

A transmissive coating polarizer has been developed for the first time; it involves the advantage of causing no light-beam deviation. The polarizer has a good transmittance ratio between the two polarization components and it incorporates filtering properties to reject the out-of-band, which might result in a better global figure of merit of a specific polarimeter if an added filter to select the Lyman α line can be avoided. The multilayer-coated transmissive polarizer could have a better performance than the classical polarizers and comparable to those of the multilayer-coated reflective polarizers when the performances of the latter are reduced by the need of a bandpass filter.

Acknowledgments

We acknowledge support by the European Community - Research Infrastructure Action under the FP6 "Structuring the European Research Area" Programme (through the Integrated Infrastructure Initiative "Integrating Activity on Synchrotron and Free Electron Laser Science"); measurements were performed under ELETTRA proposal numbers 20115134, 20120059, 20125119, 20130201, and 20135237. This work was also supported by the National Programme for Space Research, Subdirección General de Proyectos de Investigación, Ministerio de Ciencia y Tecnología, project number AYA2010-22032. L. Rodríguez-de Marcos is thankful to Consejo Superior de Investigaciones Científicas (CSIC) for funding under Programa JAE, partially supported by the European Social Fund. We also acknowledge support by the Italian Ministry of University and Research (MIUR) under the Programmi di Ricerca Scientifica di Rilevante Interesse Nazionale - Bando 2012.

References
º

[1] Fineschi S, Hoover R B, Fontenla J M, Walker A B C 1991 Polarimetry of extreme ultraviolet lines in solar astronomy Opt. Eng. **30** 1161-1168
[2] Stenflo J O, Dravins D, Whilborg N, Bruns A, Prokof'ev V K, Zhitnik I A, Biverot H, Stenmark L 1980 Search for spectral line polarization in the solar vacuum ultraviolet Solar Phys. **66** 13-20
[3] Woodgate B E et al. 1980 The Ultraviolet Spectrometer and Polarimeter on the Solar Maximum Mission Solar Phys. **65** 73-90

[4] Raouafi N -E, Lemaire P and Sahal-Bréchot S 1999 Detection of the O VI 103.2 nm line polarization by the SUMER spectrometer on the SOHO spacecraft Astron. Astrophys. **345** 999-1005
[5] Nordsieck K H, Harris W M 1999Ultraviolet astronomical polarimetry: some results and prospects Proc. SPIE **3764** 124-133
[6] West E A, Porter J G, Davis J M, Gary G A, Rabin D M, Thomas R J, Davila J M 2000 Overview of the Solar Ultraviolet Magnetograph Investigation Proc. SPIE **4139** 350-361
[7] Hardi P et al. 2011 Solar magnetism eXplorer (SolmeX) Exp. Astron. **33** 271-303
[8] Kano R et al. 2012 Chromospheric Lyman-Alpha Spectro-Polarimeter (CLASP) Proc. SPIE **8443** 84434F
[9] Metcalf H, Baird J C 1966 Circular polarization of vacuum ultraviolet light by piezobirefringence Appl. Opt. **5** 1407-1410
[10] Ott W R, Kauppila W E and Fite W L 1967 Polarization of Lyman-Alpha radiation produced in collisions of electrons and hydrogen atoms Phys. Rev. Lett. 19 1361-1363
[11] Teubner J O, Kauppila W E, Fite W I, Girnius R J 1970 Polarization of Lyman-α radiation produced in charge-transfer collisions between protons and the inert gases Phys. Rev. A **2** 1763-1767
[12] Hass G, Hunter W R 1978 Reflection polarizers for the vacuum ultraviolet using Al + MgF2 mirrors and an MgF2 plate Appl. Opt. **17** 76-82
[13] Hippler R, Faust M, Wolf R, Kleinpoppen H and Lutz H O 1985 Polarization studies of H(2p) charge-exchange excitation: H^+-Ar collisions Phys. Rev. A **31** 1399-1404
[14] Chwirot S, Chormaic S N, Dziczek D and Slevin J 1993 Efficient polarization analyzer for Lyman α radiation Appl. Opt. **32** 1583-1589
[15] Robin M B, Kuebler N A and Pao Y H 1966 Micaceous biotite as efficient Brewster angle polarizer for vacuum ultraviolet Rev. Sci. Instrum. **37** 922-924
[16] Nordsieck K H, Jaehnig K P, Burgh E B, Kobulnicky H A, Percival J W and Smith M P 2003 Instrumentation for high-resolution spectropolarimetry in the visible and far-ultraviolet Proc. SPIE **4843** 170-179
[17] Stephan G, Lemonnier J -C, Le Gavez Y and Robin S 1966 Polariseurs par réflexion pour l'ultraviolet lointain C. R. Acad. Sc. Paris Série B **262** 1272-1275

[18] McIlrath T J 1968 Circular polarizer for Lyman-alpha flux J. Opt. Soc. Am. **58** 506-510
[19] F. A. Gottwald et al. 2007 Polarization-dependent vacuum-ultraviolet reflectometry using elliptically polarized synchrotron radiation Appl. Opt. **46** 7797-7804
[20] Bridou F, Cuniot-Ponsard M, Desvignes J -M, Richter M, Kroth U and Gottwald A 2010 Experimental determination of optical constants of MgF2 and AlF3 thin films in the vacuum ultra-violet wavelength region (60–124 nm), and its application to optical designs Opt. Commun. **283** 1351-1358
[21] Bridou F, Cuniot-Ponsard M, Desvignes J -M, Gottwald A, Kroth U and Richter M 2011 Polarizing and non-polarizing mirrors for the hydrogen Lyman-α radiation at 121.6 nm Appl Phys A **102** 641–649
[22] Hamm R N, MacRae R A and Arakawa E T 1965 Polarization Studies in the Vacuum Ultraviolet J. Opt. Soc. Am. **55** 1460-1463
[23] Horton V G, Arakawa E T, Hamrn R N and Williams M W 1969 A triple reflection polarizer for use in the vacuum ultraviolet Appl. Opt. **8** 667-670
[24] Winter H, Bukow H H and Heckmann P H 1974 A high-transmission triple-reflection polarizer for Lyman-α radiation Opt. Commun. **11** 299–300
[25] Yang M, Cobet C and Esser N 2007 Tunable thin film polarizer for the vacuum ultraviolet and soft x-ray spectral regions J. Appl. Phys. **101** 053114
[26] Yang M 2007 Design and performance of a tunable polarizer for VUV and soft x-ray spectral regions J. Opt. A **9** 936–939
[27] Yang M, Cobet C, Werner C and Esser N 2008 Optical polarizer integrated with suppression of higher harmonics in the vacuum ultraviolet and soft x-ray spectral regions Appl. Phys. Lett. **92** 011110
[28] Smith N V and Howells M R 1994 Whispering galleries for the production of circularly polarized synchrotron radiation in the XUV region Nucl. Instrum. Meth. Phys. Res. A **347** 115-118
[29] Kim L, Zukic M and.Torr D G 1992 Multilayer thin film design as far ultraviolet polarizers Proc. SPIE **1742** 413-422
[30] W. C. Walker 1964 Pile-of-Plates Polarizer for the Vacuum Ultraviolet **3** 1457-1460

[31] Hinson D C 1966 State of polarization of light from a normal-incidence vacuum-ultraviolet monochromator J. Opt. Soc. Am. **56** 408
[32] Heath D F 1968 A far ultraviolet polarization analyzer for rocket use Appl. Opt. **7** 455-460
[33] Keim M, Werner A, Hasselkamp D, Schartner D -H, Lüdde H J, Achenbach A and Kirchner T 2005 Lyman-α line polarization after proton impact on atomic hydrogen J. Phys. B: At. Mol. Opt. Phys. **38** 4045–4055
[34] Winter H and Ortjohann H W 1987 High transmission polarization analyzer for Lyman-α radiation Rev. Sci. Instrum. **58** 359-362
[35] Samson J A R 1967 Polarization, chapter 9 of *Techniques of Vacuum Ultraviolet Spectroscopy*, John Wiley and Sons Inc., New York
[36] Hunter W R 2000 Polarization, in *Vacuum Ultraviolet Spectroscopy I* , J. A. Samson and D. L. Ederer, eds, Academic Press, San Diego, CA
[37] Larruquert J I 2013 Optical properties of thin film materials at short wavelengths, in *Optical thin films and coatings: from materials to applications*, A. Piegari, F. Flory, eds., Woodhead Publishing Series in Electronic and Optical Materials No. 49, Woodhead Publishing, Cambridge, UK
[38] Tolansky S 1948 Multiple-beam interferometry of surfaces and films, Oxford University Press, London
[39] Giglia A, Mahne N, Bianco A, Svetina C and Nannarone S 2011 EUV soft X-ray characterization of a FEL multilayer optics damaged by multiple shot laser beam Nucl. Instr. Meth. Phys. Res. A **635** 530-538
[40] Naletto G, Pelizzo M G, Tondello G, Nannarone S and Giglia A 2001 The monochromator for the synchrotron radiation beamline X-MOSS at ELETTRA Proc. SPIE **4145** 105-113
[41] Nannarone S et al. 2007 BEAR: a Bending Magnet for Emission Absorption and Reflectivity Notiziario Neutroni e Luce di sincrotrone, **12** 8-17
[42] Hofmann A 2004 The Physics of Synchrotron Radiation, Chapter 5, Cambridge University Press, Cambridge, UK.
[43] Fineschi S, Gardner L D, Kohl J L, Romoli M, Pace E, Corti G, Noci G 1999 Polarimetry of the UV Solar Corona with ASCE Proc. SPIE **3764** 147-160